Distance Element Performance Under Conditions of CT Saturation

Joe Mooney
Schweitzer Engineering Laboratories, Inc.

Published in the
proceedings of the 11th Annual Georgia Tech
Fault and Disturbance Analysis Conference as an alternate
Atlanta, Georgia
May 19–20, 2008

Previously presented at the
61st Annual Conference for Protective Relay Engineers, April 2008

Originally presented at the
34th Annual Western Protective Relay Conference, October 2007

Distance Element Performance Under Conditions of CT Saturation

Joe Mooney, P.E., *Schweitzer Engineering Laboratories, Inc.*

***Abstract*— Distance elements are widely used on transmission, subtransmission, and even distribution systems. Distance-based schemes are also a very economical and simple approach to protecting these lines. The ease of use of distance elements, especially in modern digital relays, has expanded the application to shorter and shorter lines. In the past it was unlikely that a distance-based scheme would be subject to CT saturation for remote fault or faults near the Zone 1 reach point. For the most part, CT saturation would occur for faults very near the relay terminal and the CT saturation would have very little impact on distance relay operation.**

This paper studies the impact of CT saturation on distance-based schemes. Saturation of the CT is evaluated for faults near to the relay location and at the reach setting. The impact to reach (underreach or overreach) and operating time are both evaluated. In addition, the behavior of directional elements is also studied. Recommendations are provided for CT sizing requirements.

I. Review of CT Saturation

Numerous papers discuss the CT theory and saturation [1, 2]. It is not the intent of this paper to review all of these concepts. However, (1) provides a criteria to avoid CT saturation:

$$20 \geq \left|\frac{X}{R}+1\right| \cdot I_f \cdot Z_b \tag{1}$$

where:

I_f is the maximum fault current in per unit of CT rating
Z_b is the CT burden in per unit of the standard burden
X/R is the X/R ratio of the fault current contribution.

Equation (1) can also be written in terms of the voltage seen by the CT secondary circuit. The left side of (1) defines a voltage rating per the ANSI standard. The same equation can be applied to a CT that uses the IEC standard to determine the voltage rating [3]. In this paper, (1) is arranged so we can determine the maximum CT secondary burden allowed such that the CT just begins to saturate. (2) is the result of arranging (1) in terms of the voltage rating, secondary current, and system X/R ratio to determine the maximum secondary burden.

$$Z_{sb} \leq \frac{V_k}{\left|\frac{X}{R}+1\right| \cdot I_{sf}} \tag{2}$$

where:

I_{sf} is the maximum secondary fault current
Z_{sb} is the CT burden in ohms secondary
X/R is the X/R ratio of the fault current contribution
V_k is the CT voltage rating.

We will use (2) as a starting point for establishing the CT sizing criteria for use with distance relays.

II. Digital Filter Response to CT Saturation

Digital, or microprocessor-based, relays use various filters to extract the fundamental frequency component of power system waveforms. Analog low-pass filters remove high-frequency components and prevent aliasing of high-frequency signals. Digital filters extract the fundamental frequency component of the voltage and current waveforms. The relays then use these digitally filtered values as phasors in such elements as distance, overcurrent, and over/undervoltage. Many papers and publications provide details on digital filter response and design [4, 5].

CT saturation causes severe waveform distortion of the secondary current supplied to the protective relays. The CT can saturate so severely that the secondary current is effectively zero [6].

Fig. 1 shows a typical current waveform associated with CT saturation. The CT used throughout this paper is a 2000/5, C800, with winding resistance of 0.76 ohms.

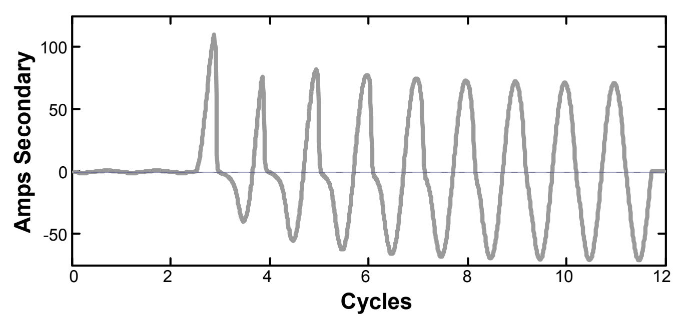

Fig. 1. Typical CT Saturation Waveform

The digital filter output resembles an ac waveform with a decrease in the peak magnitude as the CT goes into saturation. When the CT recovers from saturation, the peak magnitudes of the current waveform return to normal. Saturation of the CT also causes a phase shift between the unsaturated waveform and the saturated waveform. The phase shift may result in distance element underreach or overreach.

Fig. 2 shows saturated and unsaturated waveforms. Fig. 3 shows the saturated and unsaturated waveforms after digital filtering. Fig. 4 shows the magnitude of the filtered waveforms from Fig. 3. Finally, Fig. 5 shows the phase angle relationship between the saturated and unsaturated waveforms using the unsaturated waveform as a reference.

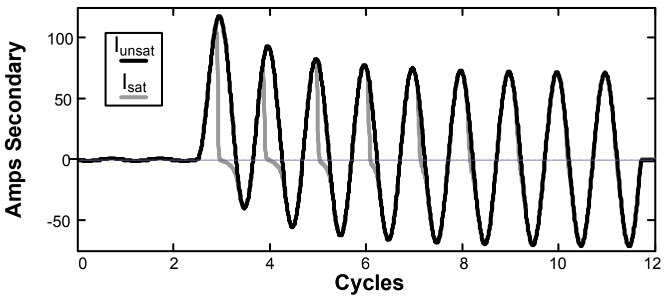

Fig. 2. Unfiltered Current Waveforms

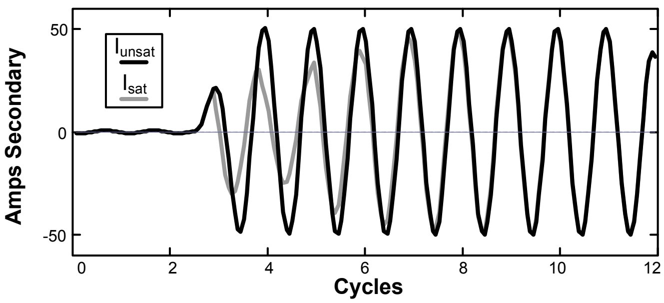

Fig. 3. Output of Full-Cycle Cosine Filter

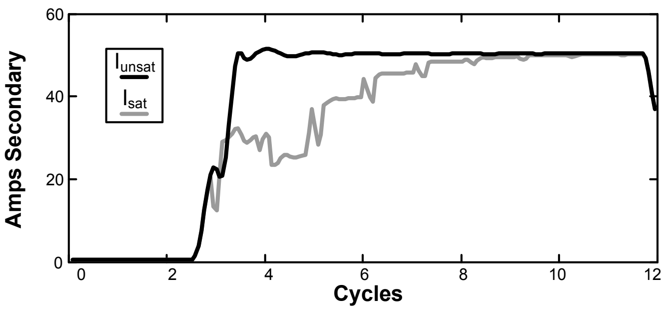

Fig. 4. Current Magnitudes With and Without Saturation

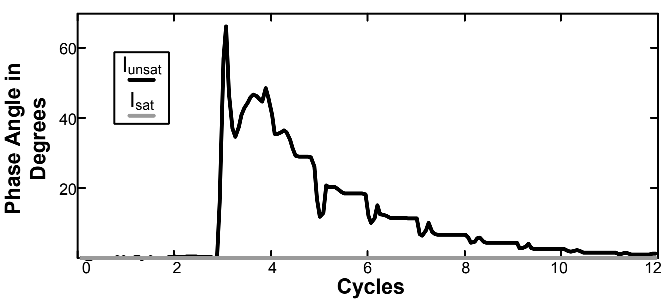

Fig. 5. Phase Relationship of Current Waveforms

III. Distance Element Review

Distance relays operate by measuring the phase relationship between an operating quantity and a polarizing quantity [7]. The operating quantity, typically known as the line-drop-compensated voltage, consists of the measured voltage, the measured current, and the reach setting. One would typically select a polarizing quantity that would be unaffected by a fault; typical polarizing quantities for mho elements are positive-sequence voltage or unfaulted phase voltage. Equation (3) shows the typical distance element operating equation. Fig. 6 shows the vector relationship.

$$P = \mathrm{Re}\left[\left(r \cdot Z \cdot I - V\right) \cdot V_P^*\right] \quad (3)$$

where:

P = Operating torque; positive is operate, negative is restrain
r = set reach
Z = replica line impedance
I = measured current
V = measured voltage
V_P = polarizing voltage

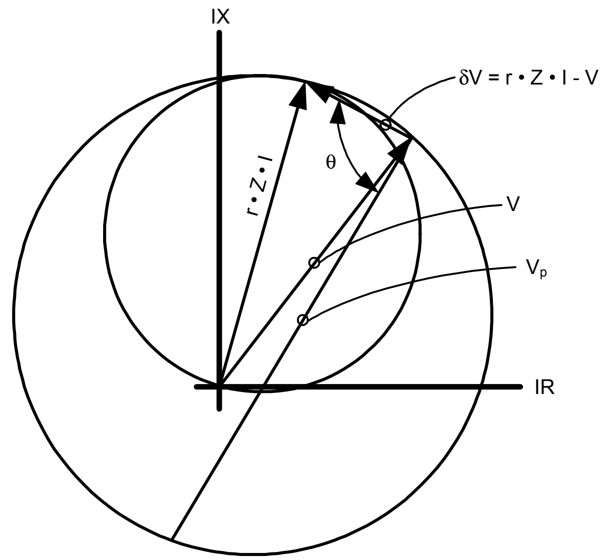

Fig. 6. Mho Element Derivation

Schweitzer and Roberts [7] proposed a novel approach in which manipulation of (3) provides a scalar output representing the term "r." This approach is computationally efficient, in that only a single calculation is necessary per fault loop. The distance element plots in the remainder of this paper use this approach. Note that when measured impedance is less than the threshold, the distance element operates. Fig. 7 shows an example plot of a fault near the Zone 1 reach.

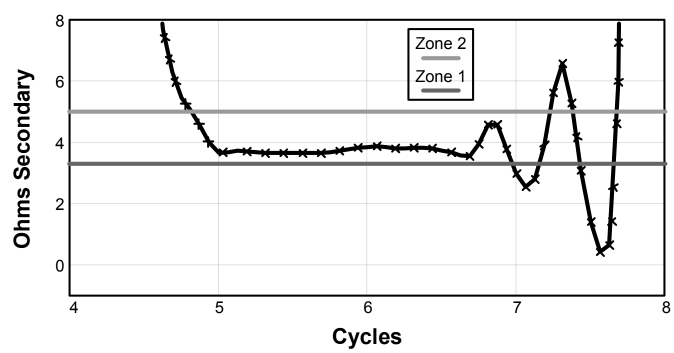

Fig. 7. Example Impedance Plot

IV. Distance Element Evaluation

This section shows the impact of CT saturation on the distance element response. A two-source system is modeled using a Real-Time Digital Simulator (RTDS®). A CT model provides secondary currents to the relay. The level of saturation varies by changing the connected burden. The system fault current level and X/R ratio remain constant.

Currents and voltages are applied from the RTDS to a popular distance relay. The output of the relay is monitored at various levels of saturation and at differing fault locations. The distance relay uses a combination of high-speed and conventional distance element algorithms [8].

Operation of the Zone 1 and Zone 2 elements are evaluated. In the case of Zone 1, the element must operate high-speed for close-in faults where CT saturation is likely to be the most severe. In addition, the Zone 1 element must meet the operating time specification provided by the manufacturer. The Zone 2 element must also operate high-speed to ensure high-speed pilot tripping. The Zone 2 element must also operate long enough to receive a permissive trip signal or time-out a blocking scheme carrier coordination delay. Backup, or time-delayed, tripping is not evaluated.

A. Reach

The Zone 1 element is set to 80 percent of the line impedance. The Zone 2 element is set to 125 percent of the line impedance. Faults are applied close-in to the relay location, at 70 percent of the Zone 1 reach setting and at the end of the line (100 percent of the line impedance).

The output of the relay is monitored for each fault condition and location. The Zone 1 element must operate for the close-in fault and the fault at 70 percent of the set Zone 1 reach. The operating time of the Zone 1 element at 70 percent of the set reach must be 0.8-cycles or less as specified by the manufacturer.

The Zone 2 element must also operate for the close-in fault. The Zone 2 element must remain picked-up for a minimum of 2.0-cycles. The 2.0-cycles requirement is determined by assuming a 1.5-cycle channel delay, 0.25-cycle input processing, and a 0.25-cycle margin for a typical permissive tripping scheme. The minimum pick-up time for a blocking scheme would typically be less.

The distance element response is plotted using a Mathcad® model of the relay that simulates digital filtering and the algorithm equations.

The maximum burden is calculated using a close-in fault. The maximum fault current is 88 amps secondary with X/R = 10. The maximum burden from (2) is then 0.82 ohms.

Fig. 8 shows output for a fault at 100 percent of the line impedance. The current transformer output is on the upper trace and the lower trace is the output of the Zone 2 distance element. The Zone 2 element operates within one-cycle and stays picked-up for at least 2.0-cycles. The secondary burden of the CT is set to 6 times the maximum burden as determined by (2).

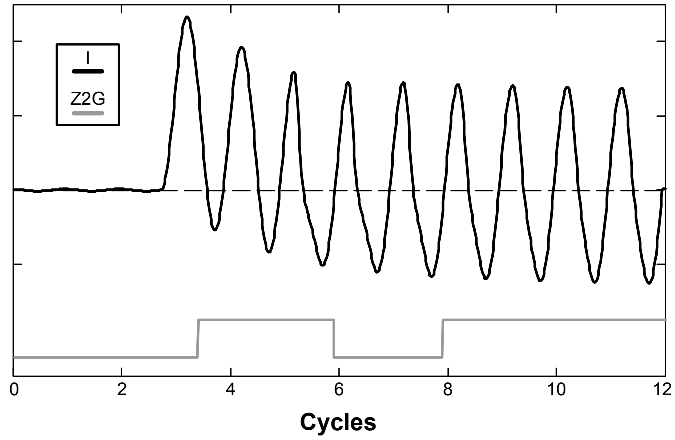

Fig. 8. Secondary Current and Zone 2 Output

Fig. 9 shows the impedance plot of the mho distance element for a fault at 100 percent of the line impedance. The dash-dot line is the Zone 2 reach setting. You can see that the measured impedance is initially less than the Zone 2 setting and is equal to the line impedance. However, as the CT begins to saturate, the measured impedance increases until it is greater than the Zone 2 setting, which results in dropout of the Zone 2 element.

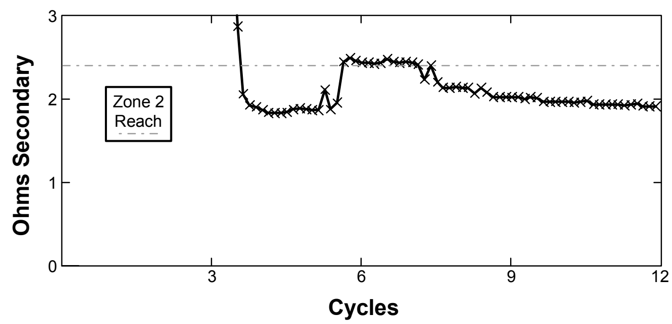

Fig. 9. Mho Element Plot

One option is to increase the Zone 2 reach setting. For example, Fig. 10 shows a Zone 2 reach setting of 200 percent of the line impedance. Extending the reach improves the distance element performance, but it may not prevent dropout of the distance element at higher levels of saturation. Fig. 11 shows the CT output for a burden equal to seven times the maximum burden. Fig. 12 shows the impedances plot with the reach set to 200 percent of the line impedance. Although the element operates correctly, you can see that the measured impedance came close to exceeding the reach setting when the CT saturated.

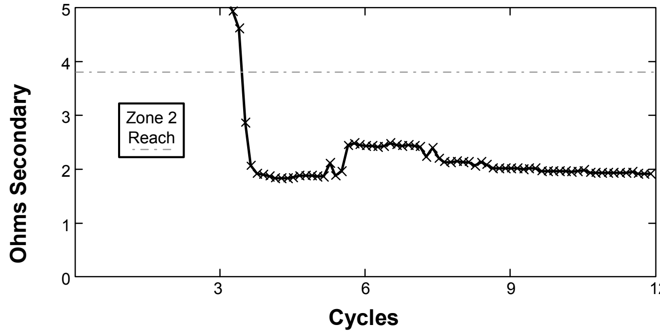

Fig. 10. Impedance Plot with Extended Zone 2 Reach Setting

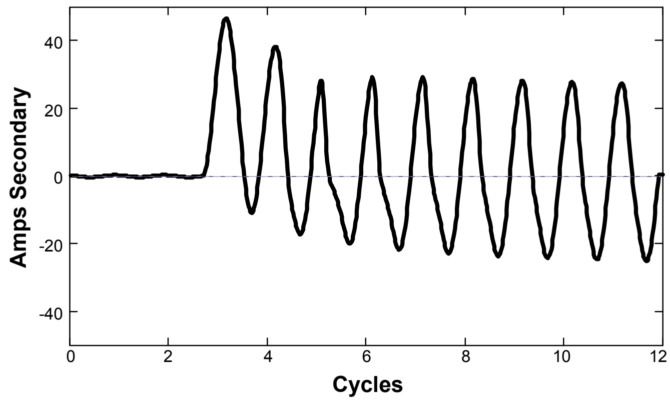

Fig. 11. Current Plot for Zb Equal to Seven Times Maximum Burden

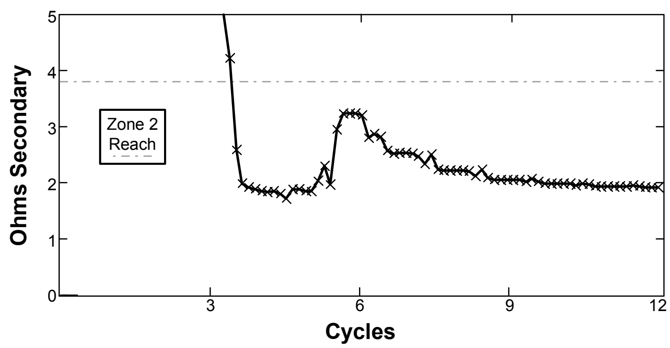

Fig. 12. Impedance Plot for Zb Equal to Seven Times Maximum Burden

Fig. 8 through Fig. 12 show that the distance element measurement is significantly impacted by the CT saturating. When the CT saturates, the measured impedance increases. As the CT recovers from saturation, the measured impedance matches that of the unsaturated plot. Therefore, the distance element appears to have a tendency to underreach, not overreach.

B. Operating Time

The operating time of a distance element can be critical to ensure high-speed tripping. When a CT saturates, it can delay operation of the distance element and result in slower than expected tripping times.

As in the previous example, the system is modeled using an RTDS and faults are applied close-in to the relay and at 70 percent of the Zone 1 element reach setting. The burden on the CT is increased until the operating time exceeds a specified value.

The design of the distance element plays a key role in how the operating time is impacted by CT saturation. One design [8], uses a combination of high-speed algorithms with conventional measurement techniques. This design operates fast under conditions of extreme CT saturation as the high-speed element can, and does, operate before the CT saturates.

The operating time tests are done with faults at 70 percent of the set reach. The operating time specified for a fault at 70 percent of the set reach is 0.8-cycles. Faults are also applied close-in to the terminal to ensure correct and secure Zone 1 operation.

Fig. 13 shows the CT output for the same burden as in the previous example — six times the calculated maximum. As the fault is close-in to the line terminal, the current magnitude is much higher and the CT saturates more severely. The lower trace in Fig. 13 is the output of the Zone 1 element. Even with CT saturation, the Zone 1 element operates in much less than a cycle and remains picked up for the duration of the fault.

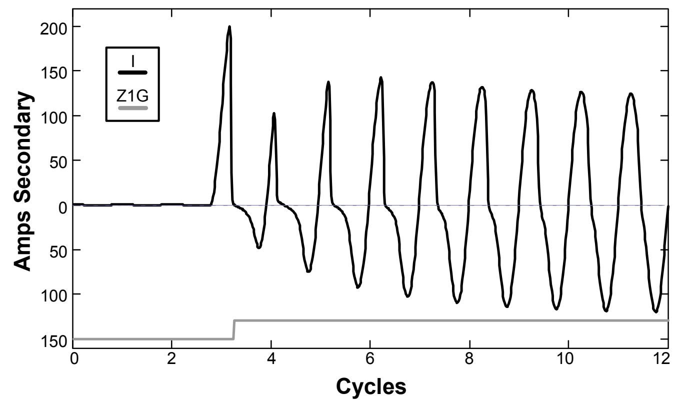

Fig. 13. CT Output and Zone 1 Operation

Fig. 14 shows the measured impedances for the high-speed algorithm and the conventional algorithm. The high-speed algorithm operates very quickly while the conventional algorithm requires more time to respond. The conventional element operates more than half-cycle after the high-speed element. The benefit of having the high-speed element is clearly illustrated in this example.

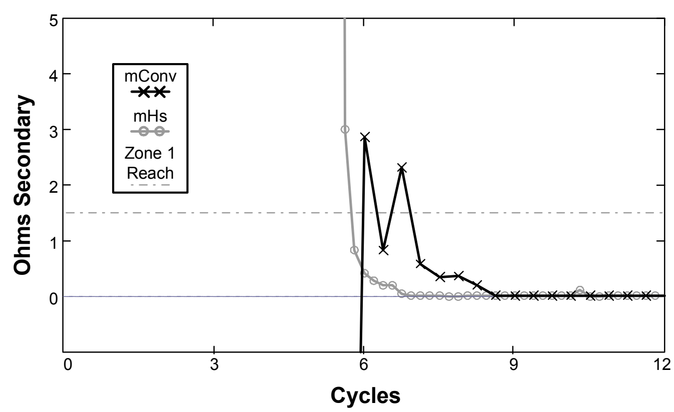

Fig. 14. Measured Impedances for High-Speed and Conventional Elements

Fig. 15 and Fig. 16 show the results for a fault at 70 percent of the set reach and CT burden set to six times the maximum. The upper trace in Fig. 15 is the output of the CT. The lower two traces are the high-speed and conventional distance element outputs. As before, the high-speed element operates very quickly; within the specified operating time of 0.8-cycles. The conventional element operates slower, but remains picked-up for a longer period of time. However, when the CT saturates, the conventional element drops out as seen in the previous examples for the Zone 2 element. But after the CT recovers, the Zone 1 element operates again. Given that the Zone 1 element is a direct tripping function with no intentional delay, the dropout of the element is not a concern.

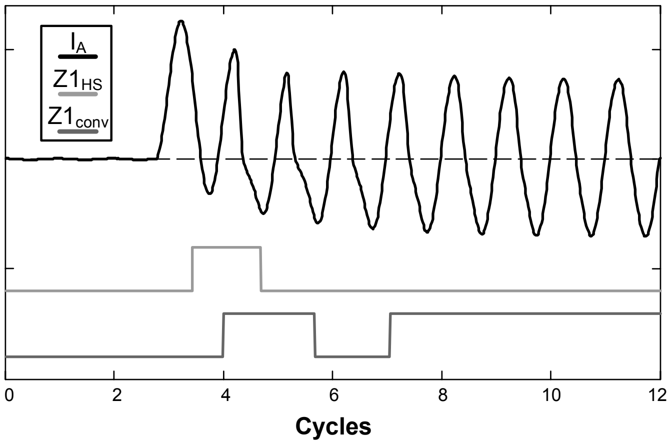

Fig. 15. CT and Distance Element Outputs for Fault at 70 Percent of Reach

Fig. 16 shows the measured impedances for the high-speed and conventional elements. As before, the high-speed element responds very rapidly, but as the CT saturates, the measured impedance increase beyond the Zone 1 setting.

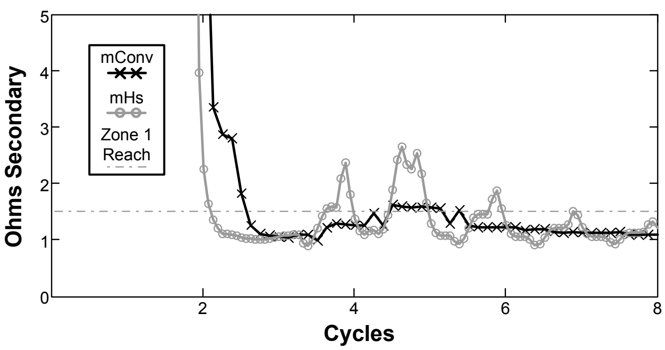

Fig. 16. Measured Impedances for Fault at 70 Percent of Reach

The high-speed distance element performs very well under conditions of CT saturation. However, there are limits to the level of saturation that can be tolerated and still provide high-speed operation. Fig. 17 shows an example of extreme CT saturation. In this case, the CT saturates very early in the first half-cycle. Because the CT is saturating so rapidly, the high-speed algorithm operates slowly; nearly 1.5-cycles.

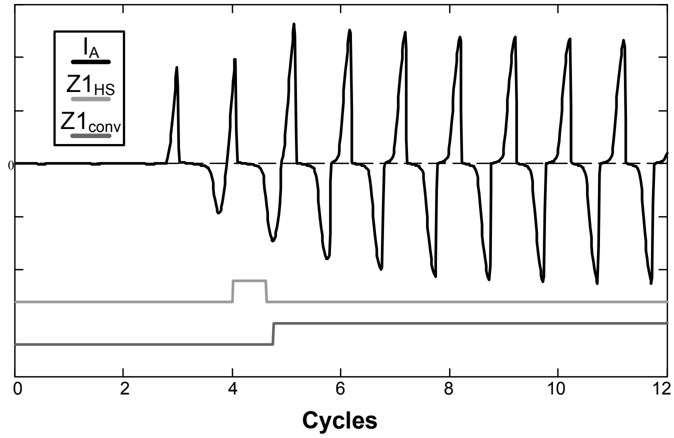

Fig. 17. Distance Element Response for Extreme Saturation

V. Directional Element Response

Directional elements are key in supervising distance and overcurrent elements. The directional element could operate incorrectly under conditions of heavy saturation. However, [9] shows that an impedance-based directional element method proposed in [7] can provide very secure operation.

As many relays use conventional torque-based directional elements, we are going to evaluate the operation of torque-based directional elements and the impedance-based technique shown in [7]. A torque-based element operates using the following formula:

$$T = |V_p| \cdot |I_o| \cdot \cos\left(\angle - V_p - \left(\angle I_o + MTA\right)\right) \quad (4)$$

where:

V_p is the polarizing voltage; typically V2 or V0

I_o is the operate current; typically I2 or I0

MTA is the maximum torque angle of the directional element.

When T is positive, the fault is in the forward direction. When T is negative, the fault is in the reverse direction.

Faults are applied directly in front of the relay location and directly behind the relay location. In both cases, the burden impedance is increased to a point where the directional element does not make correct directional decision.

Fig. 18 shows the impedance-based directional element response and Fig. 19 shows the torque-based element response. The burden is increased to 12 times the maximum calculated burden.

The directional element shown in Fig. 18 operates in the forward direction when the measured negative-sequence impedance is below the forward threshold (labeled Z2F) and reversed when above the reverse threshold (labeled Z2R). The directional element correctly indicated a forward fault. However, note that the calculated impedance comes very close to the forward threshold shortly after the fault is initiated. If the impedance moves above the Z2F line, the forward element resets. The torques-based element operated reliably in that the calculated torque is positive, indicating forward direction.

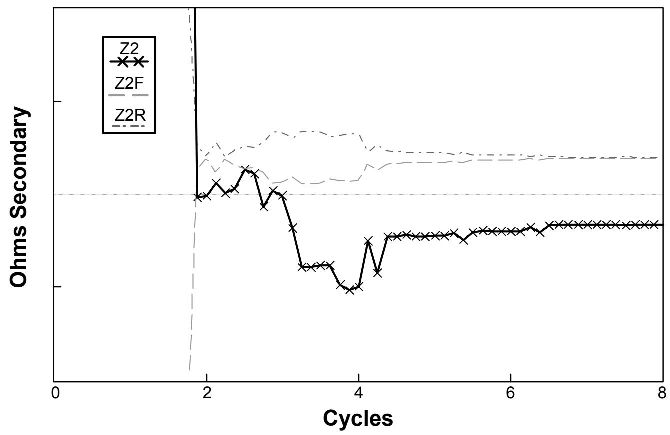

Fig. 18. Impedance-based Directional Element Response

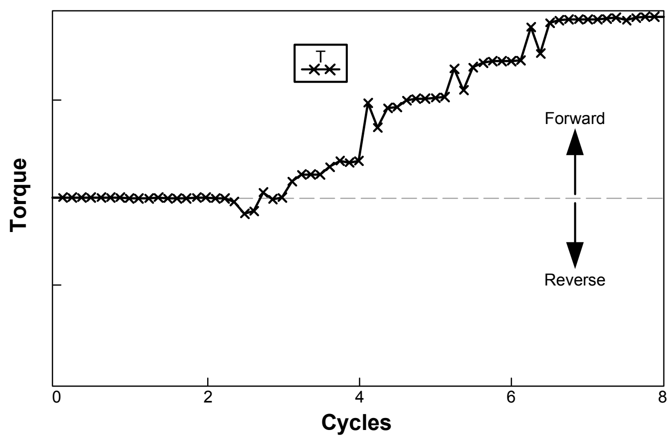

Fig. 19. Torque-base Directional Element

One benefit of the impedance-based method is that it allows compensation of the operating characteristic. Increasing the directional element threshold allows us to improve the performance of the directional element. The threshold can be increased to a value equal to or slightly greater than the line impedance as described in [7].

As with the distance element response, extreme CT saturation can result in slower operating time of the directional element. Fig. 20 shows the directional element response for a fault with extreme saturation. The directional element makes the correct directional decision, however, it is delayed.

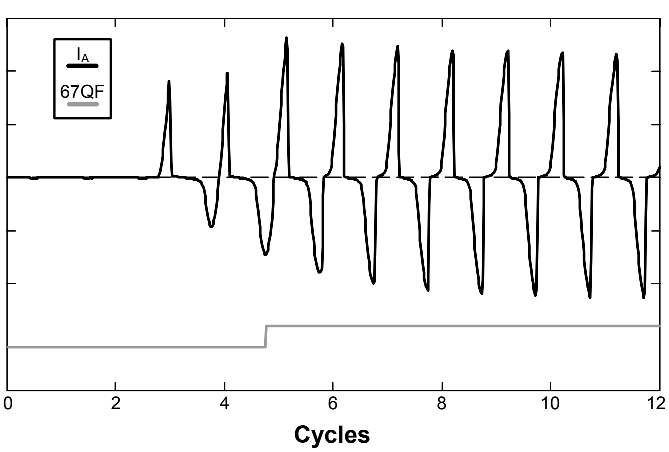

Fig. 20. Directional Element Response for Extreme CT Saturation

VI. Recommendations

Ideally, the CT should be sized so that it would not saturate for remote faults. However, in those cases where there are CT sizing restrictions and it is likely the CT will saturate for line faults, a distance element can still operate reliably. Consideration should be given to the level at which CT saturation could be experienced. Use the following criteria for specifying new CTs or for determining the suitability of an existing CT:

$$Z_{sb} \le \frac{6 \cdot V_k}{\left|\frac{X}{R} + 1\right| \cdot I_{sf}} \quad (5)$$

where:

I_{sf} is the maximum secondary fault current

Z_{sb} is the CT burden in ohms secondary

X/R is the X/R ratio of the fault current contribution

V_k is the CT voltage rating

The factor of six is selected to ensure high-speed Zone 2 operation at 100 percent of the line impedance with a Zone 2 setting of 125 percent of the line impedance. Correct operation of the Zone 2 element was the limiting factor in determining the CT sizing criteria.

Determine the maximum fault current contribution for faults near or within the Zone 1 reach. These locations will typically provide the highest level of fault current. If the connected burden is less than the right-hand side of (5), then the relay will operate correctly in terms of reach and operating time.

The directional element can tolerate extreme levels of saturation and remain secure. Using the same criteria as the distance element guarantees secure operation.

VII. Conclusions

1. CT saturation results in a reduction of the current magnitude and a phase shift in the current.
2. CT saturation results in distance element underreach and slower operating time.
3. Use (5) to ensure that the CT is sized correctly for the distance relay application. Check CT suitability at key locations, such as close-in faults or faults at the end of the line.
4. Directional elements remain secure under conditions of CT saturation. The same CT sizing criteria that applies to the distance element also applies to the directional element.

VIII. Acknowledgment

The author gratefully acknowledges the contribution of Alicia Allen. Ms. Allen, a graduate student at University of Texas–Austin and summer intern at SEL, developed the RTDS model, performed the tests, and captured the data needed to write this paper. Thank you!

IX. References

[1] Stanley E. Zocholl, Jeff Roberts, and Gabriel Benmouyal, "Selecting CTs to Optimize Relay Performance," *Proceedings of the 23rd Annual Western Protective Relay Conference*, Spokane, WA, October 1996.

[2] Stanley E. Zocholl and D.W. Smaha, "Current Transformer Concepts," *Proceedings of the 19th Annual Western Protective Relay Conference*, Spokane, WA, October 20–22, 1992.

[3] Stanley E. Zocholl, "Current Transformer Accuracy Ratings," November 2005.

[4] Joe Mooney and Satish Samineni, "Distance Relay Response to Transformer Energization: Problems and Solutions," *Proceedings of the 36th Annual Western Protective Relay Conference*, Spokane, WA, October 20–22, 2007.

[5] E. O. Schweitzer III and Daqing Hou, "Filtering for Protective Relays," *Proceedings of the 19th Annual Western Protective Relay Conference*, Spokane, WA, October 20–22, 1992.

[6] Stanley E. Zocholl and Joe Mooney, "Primary High-Current Testing of Relays with Low Ratio Current Transformers," *Proceedings of the 29th Annual Western Protective Relay Conference*, Spokane, WA, October 2003.

[7] E. O. Schweitzer III and Jeff Roberts, "Distance Relay Element Design," *Proceedings of the 19th Annual Western Protective Relay Conference*, Spokane, WA, October 20–22, 1992.

[8] Armando Guzman, Joe Mooney, Gabriel Benmouyal, and Normann Fischer, "Transmission Line Protection System for Increasing Power System Requirements," *Texas A&M Conference*, April 8–11, 2002.

[9] Ralph Folkers, "Determine Current Transformer Suitability Using EMTP Models," *Proceedings of the 26th Annual Western Protective Relay Conference*, Spokane, WA, October 1999.

X. Biography

Joe Mooney, P.E. received his B.S. in Electrical Engineering from Washington State University in 1985. He joined Pacific Gas and Electric Company upon graduation as a System Protection Engineer. In 1989, he left Pacific Gas and Electric and was employed by Bonneville Power Administration as a System Protection Maintenance District Supervisor. In 1991, he left Bonneville Power Administration and joined Schweitzer Engineering Laboratories as an Application Engineer. Shortly after starting with SEL, he was promoted to Application Engineering Manager where he remained for nearly three years. He is currently the manager of the Transmission Engineering Group of the Research and Development Division at Schweitzer Engineering Laboratories. He is a registered Professional Engineer in the states of California and Washington.

Previously presented at the 2008 Texas A&M
Conference for Protective Relay Engineers.

20070914 • TP6299-01